INTERNATIONAL JOURNAL FOR NUMERICAL AND ANALYTICAL METHODS IN GEOMECHANICS, VOL. 21, 569–579 (1997)

EQUIVALENT PROPERTIES OF ROCK STRATA: STATIC AND DYNAMIC ANALYSIS

S. V. SHESHENIN*[1], E. V. KALININ[2] AND M. I. BUJAKOV[1]

[1] *Department of Mechanics of Composites, Faculty of Mechanics and Mathematics, Moscow State University, Moscow 119899, Russia*
[2] *Department of Engineering Geology and Environment Protection, Faculty of Geology, Moscow State University, Moscow 119899, Russia*

SUMMARY

The main purpose of this investigation is to study the state of stress of layered rocks forming slopes of deep river valleys. For this purpose averaging technique and a variant of the Variation-Difference Method are used. Because of the averaging method, equivalent homogeneous properties of layered elastic medium are determined. The paper has two parts. The first one is devoted to the analysis of a static stress–strain state of the slopes under gravity. The rock mass in the second part is subjected to dynamic loading caused by an earthquake. As a result of the numerical solution of the raised problems, the stress distribution in slopes and at the base of a deep canyon-like river valley was obtained. © 1997 by John Wiley & Sons, Ltd.

Int. J. Numer. Anal. Meth. Geomech., Vol. 21, 569–579 (1997)
(No. of Figures: 4 No. of Tables: 0 No. of Refs: 15)

Key words: layered rock; heterogeneity, method of averaging, variation-difference method

1. INTRODUCTION

Investigation of Stress–Strain State (SSS) of layered rocks is of great importance in Geomechanics, for example, the construction of hydrotechnical complexes in deep canyon-like river valleys. We use Numerical Methods to evaluate SSS of natural rocks in the vicinity of a river valley. An analysis of SSS of rocks forming slopes is carried out in this paper under the assumption of a rock being elastic. The main factors that influence the distribution of stresses are the shape and the depth of the valley, heterogeneity and anisotropy of the rock. That is why Analytical Methods successfully developed for obtaining SSS in a homogeneous, generally anisotropic, elastic half-space with smooth boundary[1–6] failed to cope the problem under consideration. On the other hand, direct numerical investigation is hard if the number of layers is large enough. So the asymptotic Method of Averaging[7,8] is used. It reduces the heterogeneous problem to a homogeneous one with equivalent or the so-called effective properties. Not only average stresses but their fluctuations in layers can be obtained. To solve the boundary problem with the effective elastic properties, a variant of the Variation-Difference Method is used. For solution of the resulting linear system of algebraic equations we use combined iterative method that requires the time of computations directly proportional to the number of equations.

* Correspondence to S. V. Sheshenin, Department of Mechanics of Composites, Faculty of Mechanics and Mathematics, Moscow State University, Moscow 119899, Russia

CCC 0363–9061/97/080569–11$17.50

Received 27 April 1994
Revised 13 December 1996

The combination of the Method of Averaging and the Variation-Difference Method can be applied to the dynamical problem if the wavelength is much longer than layer width. So the last part of this paper consists of the consideration of the dynamical case. Close investigating was conducted in Reference 9. Our approach allows to obtain stress fluctuations in layers.

2. AVERAGING TECHNIQUE FOR LAYERED ROCK MASS

The stress–strain and strain–displacement relations have the form

$$\sigma_{ij} = C_{ijkl}\varepsilon_{kl}, \quad \varepsilon_{ij} = \tfrac{1}{2}(u_{i,j} + u_{j,i}), \qquad u_{i,j} \equiv \frac{\partial u_i}{\partial x_j} \tag{1}$$

where the elastic constants C_{ijkl} depend on the type of rock anisotropy and co-ordinates $\mathbf{x} = (x_1, x_2)$. The equation of motion in displacements is as follows:

$$(C_{ijkl}u_{k,l})_{,j} + \rho g\,\delta_{i2} = \rho u_{i,tt}, \quad \mathbf{x} \in V \tag{2}$$

where $\mathbf{u} = (u_1, u_2)$ is the vector of displacements, ρ is the rock density and δ_{ij} is Kronecker delta. For convenience, the familiar identical notation used in tensor calculus is employed throughout this paper to represent partial derivatives, i.e. comma denotes partial differentiation, and the subscripts i, j, t refer to co-ordinates x_1, x_2 and time. The co-ordinates x_1, x_2 are chosen along the horizontal and vertical directions (see Figure 1(a)). We assume that in the state of plane strain, all the indices $i, j, k, l, \ldots$ take the values 1, 2. Boundary conditions depend on whether static or dynamic loading is considered, therefore they are formulated separately in later sections.

As the relief of the earth may be complex, it is necessary to use a numerical method to solve the problem described by equation (2). A numerical solution is effective if the components C_{ijkl} are sufficiently smooth functions. Otherwise, for example, when the rock is bedded with a large number of beds, an averaging technique (see References 7 and 8) must be taken into account. The technique uses the idea of multiple scales. According to this idea a function of displacements is introduced as follows:

$$u_i = v_i(\mathbf{x}) + \alpha N_{ipq}(\boldsymbol{\xi})v_{p,q} \tag{3}$$

where $\mathbf{v}(\mathbf{x})$ is the smooth consistuent of the displacements, $N_{ipq}(\boldsymbol{\xi})$ is the function determining the fluctuations of the displacements in beds, α is a small parameter inversely proportional to the number of packs of beds, $\boldsymbol{\xi} = (\xi_1, \xi_2)$ are rapid co-ordinates: $\xi_i = x_i/\alpha$. Thus, we assume that the whole medium consists of repeated packs of beds. The formula (3) provides a first-order approximation with respect to α. The accuracy of the approximation (3) depends on both the beds width and the smoothness of function $\mathbf{v}$ or, in other words, on gradients $v_{p,q}$. So in many cases parameter α have not to be too small to provide good accuracy. As the extreme case, it is possible to consider only one pack of beds.

Substituting (3) into (2) we get approximation of relations (1) in first order with regard to α:

$$\varepsilon_{ij} = \tfrac{1}{2}(v_{i,j} + v_{j,i}) + \tfrac{1}{2}\left(\frac{\partial N_{ipq}}{\partial \xi_j} + \frac{\partial N_{jpq}}{\partial \xi_i}\right)v_{p,q} \tag{4}$$

$$\sigma_{ij} = P_{ijpq}v_{p,q}, \qquad P_{ijpq} = C_{ijkl}\frac{\partial N_{kpq}}{\partial \xi_l} + C_{ijpq} \tag{5}$$

In the above expressions, terms that contain α in power more than zero are thrown off. Substitution of complete expression for σ_{ij}, i.e. with terms containing α in equation (2) results in equation

$$1/\alpha \frac{\partial P_{ijpq}}{\partial \xi_j} v_{p,q} + \left(P_{ijpq} + \frac{\partial (C_{ilkj} N_{kpq})}{\partial \xi_l} \right) v_{p,qj} + \rho q \delta_{i2} = \rho v_{i,tt} + O(\alpha) \tag{6}$$

We get first-order approximation if the first term is set equal zero:

$$\frac{\partial P_{ijpq}}{\partial \xi_j} = 0, \quad p, q = 1, 2 \tag{7}$$

Averaging of (6) results in the following equation with constant coefficients:

$$H_{ijpq} v_{p,qj} + \langle \rho \rangle g \delta_{i2} = \langle \rho \rangle v_{i,tt} \tag{8}$$

where terms of order α or higher are not included. Effective moduli H_{ijkl} can be obtained as follows:

$$H_{ijkl} = \langle P_{ijkl} \rangle \tag{9}$$

where mean value $\langle \cdots \rangle$ can be taken over a pack because of the periodic structure. So function $\mathbf{v}$ can be obtained from equations (8) with corresponding boundary conditions. After we have found function $\mathbf{v}$, the displacement $\mathbf{u}$ can be obtained via formula (3) and strains and stresses in beds from the formulae (4) and (5). The functions N_{ipq} come from the solution of equation (7) in the domain of a pack of beds with conditions of periodicity and additional condition $\langle N_{ipq} \rangle = 0$. The mean stresses, strains and displacements are related by formulae

$$\langle \sigma_{ij} \rangle = H_{ijkl} \langle \varepsilon_{kl} \rangle, \qquad \langle \varepsilon_{ij} \rangle = \tfrac{1}{2} (v_{i,j} + v_{j,i} \rangle \tag{10}$$

It is easy enough to obtain functions N_{ipq} for bedded medium. In fact, in that case, the only significant component in the co-ordinate system ξ_i' is ξ_2' (Figure 1(a)) because $N_{ipq} \equiv N_{ipq}(\xi_2')$. The co-ordinate system ξ_i' is chosen so that the co-ordinate ξ_1' is directed along beds and the co-ordinate ξ_2' in the perpendicular direction. Thus, the co-ordinate system ξ_i' is turned around, relative to system ξ_i, on the angle θ (see Figure 1(a)). In this case equation (7) transforms into the ordinary differential equation

$$\frac{\mathrm{d}}{\mathrm{d}\xi_2'} \left(C'_{i2k2} \frac{\mathrm{d}N'_{kpq}}{\mathrm{d}\xi_2'} + C'_{i2pq} \right) = 0, \quad p, q = 1, 2 \tag{11}$$

that have to be added with the condition of periodicity: $N'_{kpq}(0) = N'_{kpq}(l_p)$, where (l_p) is the width of the pack. The mean value over the pack of function $f(x, \xi_2')$ is determined by formula $\langle f \rangle(x) = \int_0^{l_p} f(x, \xi_2') \, \mathrm{d}\xi_2'$. In the co-ordinate system ξ_i' functions N'_{kpq}, P'_{ijnk} obtained from the equation (11) can be expressed as follows:

$$N'_{kpq}(\xi_2') = C'^{-1}_{k2i2} \langle C'^{-1}_{i2m2} \rangle^{-1} \langle C'^{-1}_{m2n2} C'_{n2pq} \rangle - C'^{-1}_{k2i2} C'_{i2pq} \tag{12}$$

$$P'_{ijnk}(\xi_2') = C'_{ijnk}(\xi_2') + C'_{ijm2}(\xi_2') \times [C'^{-1}_{m2l2}(\xi_2') \langle C'^{-1}_{l2p2} \rangle^{-1} \langle C'^{-1}_{p2q2} C'_{q2nk} \rangle - C'^{-1}_{m2l2}(\xi_2') C'_{l2nk}(\xi_2')] \tag{13}$$

Here C'^{-1}_{k2i2} means the inverse of the matrix C'_{k2i2} and so for other matrixes in expressions (12) and (13).

At the end of this section, we consider the bedded medium of identical beds with thin soft interlayers between them. A model for such material is a bedded medium with linear contact conditions along the beds' boundaries

$$\sigma'_{12} = k[u'_1]$$

where square brackets denote the value of the tangential displacement jump. The coefficient k is equal to μ/δ, where δ and μ are, respectively, an interlayer's width and shear elastic modulus. Averaging procedure applied to such a medium shows that the effective moduli are the same as the bed's, except for the modulus $H'_{1212} = (C'^{-1}_{1212} + k^{-1})^{-1}$ which differs from the bed's shear modulus C'_{1212}. Components of tensors **H**, **P**, **N** in the co-ordinate system ξ_1, ξ_2 can be obtained by tensor analysis rules.

3. ANISOTROPIC ROCK UNDER GRAVITY

In this section we consider the rock mass forming the domain V (see Figure 1(a)) and subjected to gravity. The model of the rock's equilibrium is described by equation (8) with zero instead of the inertial term on the right-hand side and the following boundary conditions:

$$H_{ijkl} v_{k,l} n_j = 0, \quad \mathbf{x} \in \Sigma_2 \tag{14}$$

$$H_{ijkl} v_{k,l} n_j \tau_i = 0, \quad v_i n_i = 0, \quad \mathbf{x} \in \Sigma_1 \tag{15}$$

where $\mathbf{n}$ is the unit vector of external normal to Σ, $\boldsymbol{\tau}$ the unit vector tangential to Σ and $\Sigma = \Sigma_1 + \Sigma_2$ is the boundary of the two-dimensional domain V.

Briefly, the numerical algorithm is developed as follows. Coming from the variational equation equivalent to the problem (8), (14), (15), by use of the Variation-Difference Method on curvilinear mesh, we obtain the system of linear equations:

$$\mathbf{A}^h \mathbf{v}^h + \mathbf{F}^h = 0 \tag{16}$$

that approximates the system (8), (14), (15). The details of the method are described in References 10 and 11. In Reference 10 such a method is called 'the method of external approximation'.

To solve the system (16), a preconditioned Combined Iterative Method (CIM) was suggested (see Reference 11). The method is composed of Gradient Method and the two-row Chebyshev method. It proves to be possible to find approximations to the eigenvalues of the preconditioned matrix A^h in the end of the first stage of the CIM. It can be shown that after a few gradient iterations their convergence rate decreases deeply and equals to a constant value. After that the eigenvalues can be found as roots of a quadratic equation (see Reference 12). In the second stage of the CIM, i.e. during Chebyshev iterations we use eigenvalues adaptation (see Reference 13) to improve convergence rate. Preconditioning matrix was chosen as the finite-difference Laplace operator on a rectangular grid. It was proved that Laplace matrix is spectrally equivalent to the matrix A^h. Therefore, the convergence rate does not depend on the discretization parameter h. We used fast direct methods, e.g. Marching Algorithms [14] to solve the finite-difference Laplace equation. So the total number of arithmetic operations required for CIM is in a direct proportion

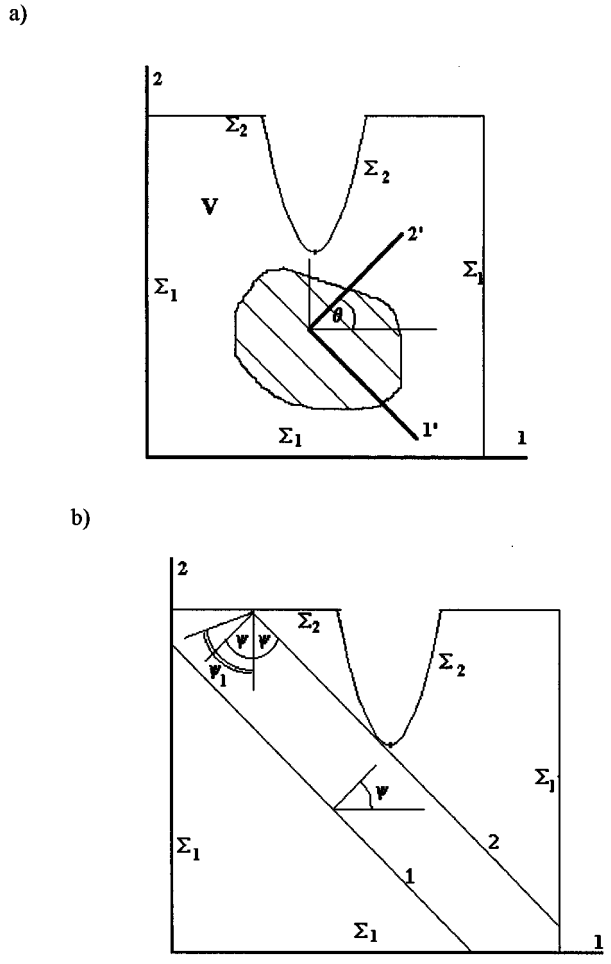

Figure 1. The analysed domain formed by dipped bedded rocks, with a symmetrical cut (a) and the scheme of propagation of a plane wave (b). The dimensions of the domain are 3 km in both directions, Cut's depth is about 1 km, width equals 700 m

to the number of equations. So is the time of computations. This fact was tested for systems up to 40,000 equations. Besides this the advantage of the CIM is its stability to round-off errors. That is why the CIM allows to solve system with a high condition number.

4. SSS IN BEDDED MEDIUM UNDER PRESSURE OF BASEMENT

In this section we give the comparison of two solutions obtained directly by numerical approximation of the heterogeneous problem and with the help of asymptotic technique. For the purpose of comparison, the boundary problem shown in Figure 2 is chosen. In this problem the influence of gravity was not taken into account, so the bedded medium was subjected only to the basement pressure. In this example, the pack of layers consists of two layers of equal width l so that

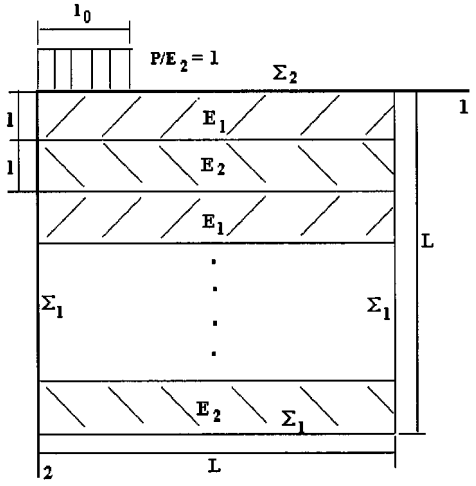

Figure 2. The bedded medium under the pressure of basement. The part of the boundary Σ_2 on the right of the basement is free of stresses. Along the part of the boundary Σ_1 normal displacement and tangential stress are equal zero. Only one-half of the whole domain V is used in computations because axis x_2 is the axis of horizontal symmetry

$l_p = 2l/L$. The number of packs equals 8 and $l/l_0 = 1{\cdot}25$ (see Figure 2 for details). The materials of first and second layers are sand and clay with Young's moduli ratio: $E_1/E_2 = 4$, $\nu_1 = 0{\cdot}3$, $\nu_2 = 0{\cdot}4$. Figure 3(a) shows the graph of σ_{22}/P: dashed line corresponds to direct numerical solution, solid line to average stress σ_{22}, obtained by first formula (10). The same explanation is applied to Fig. 3(b) that represents the fluctuations of strain $\varepsilon_{22}/(P/E_2)$, which is discontinuous function.

Also the influence of approximation of infinite semi-plane by finite domain was explored. The ratio of L/l_0 was chosen to be 10 and 20. The SSS in the half of the smaller domain was almost identical to the solution in the larger domain.

5. SSS UNDER GRAVITY—THE NUMERICAL RESULTS

The method presented was used to assess the SSS of medium consisting of periodically interbedded isotropic beds of rocks with different elastic properties. We considered the case when the rock consisted of two periodically interbedded isotropic beds of approximately equal thickness. The Young's modulus of the more rigid bed was $E_1 = 10^4$ MPa, Poisson's ratio $\nu_1 = 0{\cdot}3$; for the softer bed $E_2 = 10^3$ MPa, $\nu_2 = 0{\cdot}4$. The relief shown in Figure 1 is an approximation of deep and narrow canyon-like river Narin walley in Kirgizia. The lowest 500 m of the valley almost exactly coincides with chosen approximation. At the top, the real valley is wider than the one in our example. So stresses near the bottom of the valley should be higher in our computations than in reality. The bed's width was taken equal to 1 m. The distribution of vertical stress σ_{22} in rigid and soft beds is shown in Figure 4.

As a rule, the magnitude of stress in rigid beds in higher than in soft beds. The pattern of stress distribution and the order of their magnitudes in rigid beds are almost the same as in the case of anisotropic rock with the effective properties. The concentration of horizontal stress in soft beds was found near the bottom of the valley where the beds dip into the slope. There is a concentration of vertical stresses in the same part of the valley, and there are tensile vertical stresses at the

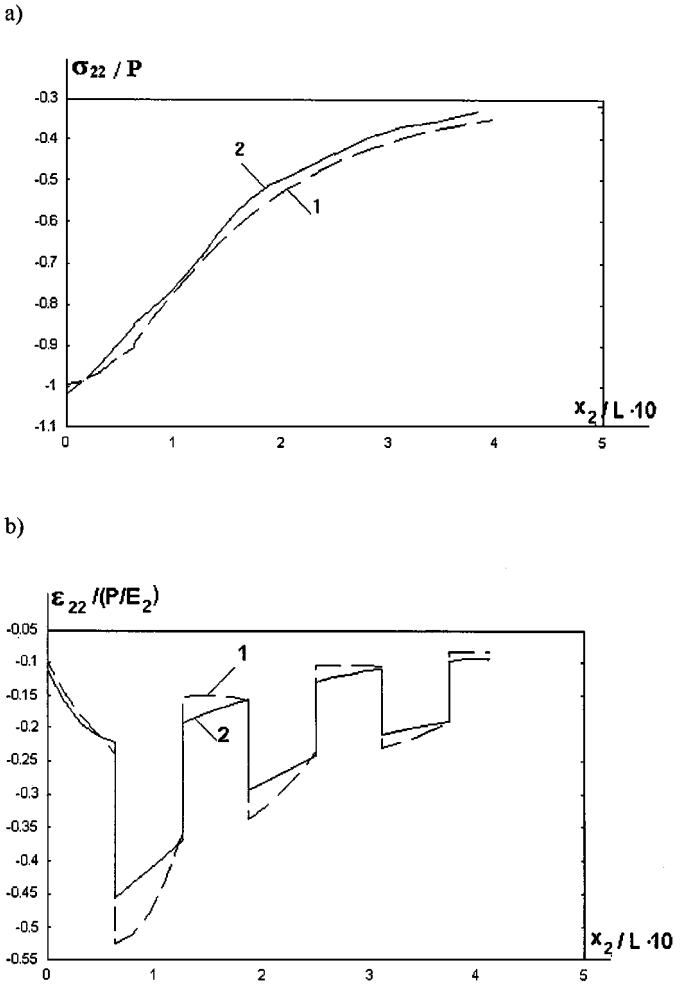

Figure 3. The graphs of (a) vertical stress σ_{22} and (b) vertical strain ε_{22} along vertical axis x_2 ($x_1 = 0$). Solid line represents asymptotic solution when dash line corresponds to direct one

lowest point of it. Tangential stress also reaches a maximum there, and the line of zero tangential stresses goes through the lower part of the valley from the side where the dip of rocks or jointing is parallel to the slope. Thus, most of the investigated area has single-directed shear.

Certainly, a medium consisting of periodically repeated two-layered pack is only an approximation of a real rock. The same computations were made for another model that treated rock as a bedded medium of identical beds with thin soft interlayers between them.

6. ROCKS UNDER DYNAMIC LOAD

Now, we consider propagation of weak seismic waves through the rock mass in vicinities of a canyon (Figure 1(b)). Averaging technique described in Section 2 in the case of sufficiently long

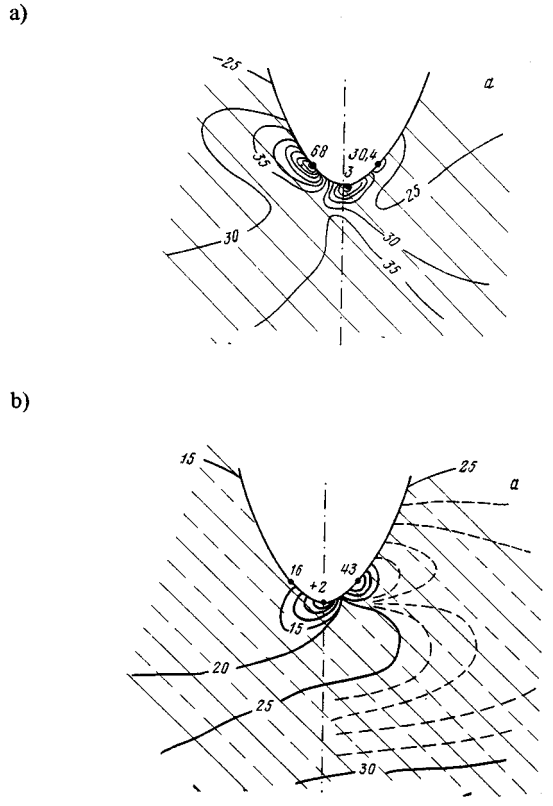

Figure 4. The distribution of vertical stress σ_{22} (MPa) near the base of the valley in (a) rigid and (b) soft beds of the heterogeneous rock (1 cm in the diagrams stands for approximately 100 m in reality)

waves as compared to the bed's width results in equation (8). The boundary condition (14) also can be accepted to the boundary's portion Σ_2. The more difficult task is to formulate the boundary conditions along Σ_1 because of the need to use an analytical solution of the problem on a plane wave reflection at a horizontal flat boundary. The use of exact solution along the 'artificial' boundary Σ_1 prevents from any error in cutting the finite domain V from the infinite semi-plane, which is true until the boundary conditions along Σ_1 are true, i.e. until the wave reflected at canyon's slope reaches the 'artificial' boundary Σ_1.

Let a plane *p*-wave propagate from the left bottom corner of the domain as shown in Figure 1(b). (We do not deal with Rayleigh's waves in this study.) If the first front's locations is the line '1' in Figure 1(b) at some instant, then the displacements in the part of the boundary Σ_1 below the front can be determined from the analytical formulae for plane wave (see Reference 15 for details): If the first front of the *p*-wave has advanced to the location '2' in Figure 1(b), then it is necessary to add expressions for displacements generated by the waves reflected from the left horizontal part of the boundary Σ_2. Angle ψ denotes the angle between the horizon and the direction of propagation of the *p*-wave, the same angle is between the horizon and the *pp*-wave's direction, ψ_1 is the angle for the *psv*-wave.

The displacements in the remaining part of the boundary Σ_1 are equal to zero. Thus, the boundary condition along the boundary Σ_1 is the displacements determined by analytical formulae and can be written in the form

$$\mathbf{v}_{|\Sigma_1} = \mathbf{v}_\Sigma(\mathbf{x}, t) \tag{17}$$

where $\mathbf{v}_\Sigma$ is a given function. The initial condition behind the first front of the p-wave is stated analytically in the same way as that of the boundary, and the displacements before the first front are equal to zero. On the whole, one can write out

$$\mathbf{v}(\mathbf{x}, t)_{|t=0} = \mathbf{U}^0(\mathbf{x}), \frac{\partial \mathbf{v}(\mathbf{x}, t)}{\partial t} | t = 0 = \mathbf{V}^0(\mathbf{x}) \tag{18}$$

So, the formulae (8), (14), (17) and (18) describe a boundary value problem in terms of displacements in the domain V.

The following numerical method was used to solve the problem (8), (14), (17) and (18). The discretization of the left-hand side of equation (8) with boundary conditions (14) and (17) is carried out just as described in Section 3. The second-order partial derivative on the right-hand side of approximated by the expression $(\mathbf{u}^{m+1} - 2\mathbf{u}^m + \mathbf{u}^{m-1})/\tau^2$ with the second-order accuracy (denoted $t_m = m\tau$, $\mathbf{u}^m = \mathbf{u}(\mathbf{x}, t_m)$). So we can write out the explicit difference equation approximating (8), (14) and (17):

$$\mathbf{A}^h \mathbf{v}^{h,m} + \mathbf{F}^h = \langle \rho \rangle \frac{(\mathbf{v}^{m+1} - 2\mathbf{v}^m + \mathbf{v}^{m-1})}{\tau^2} \tag{19}$$

where the matrix $\mathbf{A}^h$ is the difference operator that is introduced in (16).

A series of accuracy tests was done.

(A) In the state when the analytical solution existed (first front locations to the left and below the line '2' in Figure 1(b)) the difference between the exact and computed values of displacements was investigated. To estimate the error, one could start numerical computation at 300τ, or 200τ, or 3τ since the first front entering the domain and halt at 350τ, when the analytical solution was still valid. It was stated that the error appeared in this test during the period equal to that of the actual computation (i.e. nearly 100τ) was less than 5 per cent in the interior of the disturbed portion, and 15 per cent along the edge of the first front, where the derivatives of the displacements are discontinuous. It was also tested that the error did not increase significantly after 100 steps of the numerical computation in this test.

(B) In the same setup as above, the error in the stress values was evaluated. It appeared to be 10 per cent of the magnitude of the global maximum.

7. DISCUSSION ON THE RESULTS OF NUMERICAL COMPUTATION

The analytical solution that we used as boundary condition along the boundary's part Σ_1 was valid only for isotropic medium. So further consideration concerns that case.

The constants of the rock in the domain V are specified as follows: the Young's modulus $E = 5(10^4)$ MPa, the Poisson's ratio $\nu = 0{\cdot}29$, the density of rock $\rho = 3$ g/cm^3. The parameters of

the seismic wave correspond to a small earthquake: the frequency is 5 Hz, the amplitude of the *p*-wave $A = 0{\cdot}1$ cm; its velocity $c = 4600$ m/s; the wave length is 920 m, the explored angles between the horizon and the direction of the *p*-wave's propagation were 20, 45 and 70°. The time step for numerical computation τ equals $1{\cdot}37(10^{-3})$ s.

The wave was chosen of a sinusoidal shape behind the first front with discontinuity of displacement derivatives along the edge of the front. There was also an attempt to smooth the derivatives using the form of $\sin^2$ for the first-quarter of the period of the *p*-wave.

The solution obtained allows us to follow the evolution of the stress field during the time equal to nearly one wave period, to locate the zones of stress concentration and to discover their dependence on the angle of the *p*-wave's direction. The stress values caused by the interference with the surface are comparatively small and do not exceed 1 MPa which is three times greater than those produced by the *p*-wave in the continuum of the rock.

Below we describe the stress intensity field in the case when the *p*-wave's vector is at 45° to the horizon. The two main zones of stress concentration are being formed at the initial stage of the wave hitting the surface of the valley and the reflected waves generation: one due to frontal impact at the left slope, and the other near the bottom of the canyon, at the point where the front of the *p*-wave constitutes the right angle with the surface of the canyon. After that, the first zone of high stress moves upwards along the slope, and there is an increase in the stresses in the second zone. When the disturbance fully confines the whole canyon, the zone of highest stress concentrations moves toward the top of the slope where the interference of waves reflected from both the slope and the flat portion of the top boundary occurs, while the stress in the second zone diminishes to a nominal value. In a half-period a new zone of increased stress starts to form, and the process repeats. It is noticed that both highest tension-compression and shear stress components are localized in the same areas, as the stress intensity shown.

8. CONCLUSIONS

The mathematical apparatus described allows to reduce the task of estimating the SSS in bedded heterogeneous rocks to the same task for anisotropic rock both in static and dynamic cases. The proposed methods for evaluating the SSS of solids are realized as a software in FORTRAN. The data obtained as a result of using the proposed methods indicate that the structure of rocks, which is determined by bedding, rock properties, their occurrence and jointing, to a considerable degree influence the value and the pattern of the stress distribution in the rock.

REFERENCES

1. B. Amadei, W. Z. Savage and H. S. Swolfs, 'Gravitational stress in anisotropic rock masses', *Int. J. Rock Mech. Min. Sci. Geomech. Abstr.*, **24,** 5–14 (1987).
2. D. F. McTigne and C. C. Mei, 'Gravity-indiced stresses near axisymmetric topography of small slope', *Int. J. Num. Anal. Methods Geomech.*, **11,** 257–268 (1987).
3. J. J. Liao, W. Z. Savage and B. Amadei, 'Gravitational stress in anisotropic ridges and walleys with small slopes', *J. Geophys. Res.*, **97,** 3325–3336 (1992).
4. B. Amadei and E. Pan, 'Gravitational stress in anisotropic rock masses with inclined strata', *Int. J. Rock Mech. Min. Sci. Geomech. Abstr.*, **29,** 225–236 (1992).
5. E. Pan, B. Amadei, 'Gravitational stresses in long asymmetric ridges and valleys in anisotropic rock', *Int. J. Rock Mech. Min. Sci. Geomech. Abstr.*, **30,** 1005–1008 (1993).
6. E. Pan and B. Amadei, 'Stresses in an anisotropic rock mass with irregular topography', *ASCE J. Eng. Mech.*, **120,** 97–119 (1994).

7. N. S. Bachvalov and G. P. Panacenko, *Homogenization, Averaging Processes in Periodic Media. Mathematical Problems in the Mechanics of Composite Materials*, Kluwer Academic Publishers, Dordrecht 1989.
8. B. E. Pobedria, *Mechanics of Composite Materials*, Moscow University Press, Moscow, 1984 (in Russian).
9. A. Papageorgiou and J. Kim, 'Propagation and amplification of seismic waves in 2-D valleys excited by obliquely incident P- and SV-waves', *Earthquake eng. struct. dyn*, **22,** 167–182 (1993).
10. R. Glovinski, J. L. Lions and R. Tremolieres, *Analyse numerique des inéqualions variotionnelles*, Dunod, Paris, 1976.
11. B. E. Pobedria, S. V. Sheshenin and T. Holmatov, *Boundary Problems in Terms of Stress*, FAN, Tashkent, 1988 (in Russian).
12. A. A. Samarskiy and E. S. Nikolaev, Numerical Methods for Grid Equations, Birkhauser, Basel, 1987.
13. L. A. Hageman and D. M. Young, *Applied Iterative Methods*, Academic Press, A Subsidiary to Harcout Brace Jovanovich Publishers, New York, 1981.
14. R. E. Bank, Marching algorithms for elliptic boundary value problems, *Doctoral thesis*, Harvard Univ., Cambridge, MA. 1975.
15. E. F. Savarenskii and D. P. Kirnos, *Elements of Seismology and Seismometry*, Moscow, 1955 (in Russian).

